Loads Analysis of Several Offshore Floating Wind Turbine Concepts

A.N. Robertson and J.M. Jonkman

NOTICE

The submitted manuscript has been offered by an employee of the Alliance for Sustainable Energy, LLC (Alliance), a contractor of the US Government under Contract No. DE-AC36-08GO28308. Accordingly, the US Government and Alliance retain a nonexclusive royalty-free license to publish or reproduce the published form of this contribution, or allow others to do so, for US Government purposes.

This report was prepared as an account of work sponsored by an agency of the United States government. Neither the United States government nor any agency thereof, nor any of their employees, makes any warranty, express or implied, or assumes any legal liability or responsibility for the accuracy, completeness, or usefulness of any information, apparatus, product, or process disclosed, or represents that its use would not infringe privately owned rights. Reference herein to any specific commercial product, process, or service by trade name, trademark, manufacturer, or otherwise does not necessarily constitute or imply its endorsement, recommendation, or favoring by the United States government or any agency thereof. The views and opinions of authors expressed herein do not necessarily state or reflect those of the United States government or any agency thereof.

Available electronically at http://www.osti.gov/bridge

Available for a processing fee to U.S. Department of Energy
and its contractors, in paper, from:

       U.S. Department of Energy
       Office of Scientific and Technical Information

       P.O. Box 62
       Oak Ridge, TN 37831-0062
       phone: 865.576.8401
       fax: 865.576.5728
       email: mailto:reports@adonis.osti.gov

Available for sale to the public, in paper, from:

       U.S. Department of Commerce
       National Technical Information Service
       5285 Port Royal Road
       Springfield, VA 22161
       phone: 800.553.6847
       fax: 703.605.6900
       email: orders@ntis.fedworld.gov
       online ordering: http://www.ntis.gov/help/ordermethods.aspx

Cover Photos: (left to right) PIX 16416, PIX 17423, PIX 16560, PIX 17613, PIX 17436, PIX 17721

Printed on paper containing at least 50% wastepaper, including 10% post consumer waste.

Loads Analysis of Several Offshore Floating Wind Turbine Concepts

Amy N. Robertson and Jason M. Jonkman
National Renewable Energy Laboratory
Golden, CO, USA

ABSTRACT

This work presents a comprehensive dynamic-response analysis of six offshore floating wind turbine concepts. Each of the six models contained the same 5-megawatt (MW) turbine. The platforms modeled included: a barge, a semisubmersible, two tension-leg platforms (TLP), and a spar buoy at two different depths. The performance of these models was compared to that of a base model with a turbine supported by a fixed land-based tower. Performance was evaluated via a comprehensive loads and stability analysis adhering to the procedures of the International Electrotechnical Commission (IEC) 61400-3 offshore wind turbine design standard. The loads in the turbine supported by the barge are the highest found for the floating concepts. The differences in the loads between the TLP, the semisubmersible, and the spar buoy are not significant, except for the loads in the tower, which are greater in the spar and semisubmersible systems. The results of this analysis will help resolve the fundamental design trade-offs between the floating-system concepts.

KEY WORDS

Offshore wind turbine; aero-hydro-servo-elastic analysis; tension leg platform; spar buoy; barge; semisubmersible

INTRODUCTION

Currently, most offshore wind turbines are installed in shallow water on bottom-mounted substructures. These substructures include gravity bases and monopiles used in water to about 30-meter (m) depth and space-frames—such as tripods and lattice frames (e.g., "jackets")—used in water to about 50-m depth. In contrast, harnessing much of the vast offshore wind resource potential of the USA, China, Japan, Norway, and many other countries requires installations to be located in deeper water. At some depth, floating support platforms will be the most economical type of support structure to use.

Numerous floating support-platform configurations are possible for use with offshore wind turbines, particularly when considering the variety of mooring systems, tanks, and ballast options used in the offshore oil and gas (O&G) industry. The platforms, however, can be classified in terms of how they achieve basic static stability in pitch and roll. The three primary concepts are: the TLP, which maintains stability primarily through the mooring system and excess buoyancy; the spar buoy, which maintains stability from a deep draft combined with ballast; and the barge, which uses a large waterplane area and shallow draft to maintain stability. Hybrid systems use a combination of these three stability methods. For instance, a semisubmersible is a hybrid concept that relies on large waterplane area as well as a fairly deep draft and ballasting to maintain stability.

To help understand the fundamental design trade-offs between the different concepts, a quantitative comparison is made between the dynamic responses of a variety of floating wind systems. This paper examines six floating systems, and compares their performance to a wind turbine on land. Three of the floating systems have been examined previously in Jonkman and Matha 2010, and the other three are generic systems created for a demonstration project led by the DeepCwind consortium (www.deepcwind.org) based out of the University of Maine (see DeepCwind). The original three concepts include the MIT/NREL TLP, the OC3-Hywind Spar, and the ITI Energy Barge, which incorporates a concept from each of the three primary stability categories. The three new concepts created for the University of Maine project include the UMaine TLP, the UMaine-Hywind Spar, and the UMaine semisubmersible. Both the TLP and semisubmersible are very different from the original MIT/NREL TLP and barge, but the spar remained the same. The only difference between the UMaine-Hywind Spar and the OC3-Hywind Spar is the water depth in which the design was analyzed. All University of Maine designs are analyzed at a water depth of 200 m, which represents the depth of a test site for floating wind turbines off the coast of Maine.

OVERVIEW OF THE ANALYSIS APPROACH

The overall design and analysis process applied in this project consists of the following steps:

1. Use the same wind turbine specifications—including specifications for the rotor, nacelle, tower, and controller—for each system. (Minor modifications to the specifications are needed in some cases; see Step 2.) Likewise, use the same environmental conditions for each analysis—including meteorological (wind) and oceanographic (wave), or "metocean," parameters. Using the same

wind turbine specifications and metocean data for all analyses enables an "apples-to-apples" comparison of the systems.

2. Determine the properties of each floater, including the platform and mooring system designs. To be suitable, each floating platform must be developed specifically to support the rotor, nacelle, and tower of the wind turbine. In some cases, the wind turbine tower might need to be modified in this step to ensure conformity to the platform (while maintaining the same hub height). Some platforms also require adaptation of the wind turbine control system in this step to avoid controller-induced instabilities of the overall system. For an explanation of the potential instabilities, see Larsen et al. 2007 and Jonkman 2007.

3. Develop a model of each complete system within a comprehensive simulation tool capable of modeling the coupled dynamic response of the system from combined wind and wave loading.

4. Using each full system dynamics model from Step 3, perform a comprehensive loads analysis to identify the ultimate loads and fatigue loads expected over the lifetime of the system. Loads analysis involves running a series of design load cases (DLC) covering essential design-driving situations, with variations in external conditions and the operational status of the turbine. The loads are examined within the primary components of the wind turbine, including the blades, drivetrain, nacelle, and tower—and for the floating system, the mooring lines. Potential unexpected instabilities also can be found in this process.

5. Using the results of Step 4, characterize the dynamic responses of the land- and sea-based systems. Comparing the land-based and sea-based systems responses enables quantification of the impact brought about by the dynamic coupling between the turbine and each floating platform in the presence of combined wind and wave loading. Comparing the responses of the six sea-based systems with each other enables quantification of the impact of the platform configuration on the turbine.

The "Overview of the Analysis Specifications" section describes the specifications, data, and procedures used in this project for Step 1, Step 2, and Step 4. The capabilities of the simulation tool used for this project (Step 3) are described in the following section. The results of Step 4 and Step 5 are presented in the "Results and Discussion" section.

SIMULATION TOOL CAPABILITIES

This work applies the NREL-developed FAST servo-elastic tool (Jonkman, 2005), coupled with the AeroDyn rotor aerodynamics module (Laino, 2002) and HydroDyn platform hydrodynamics module (Jonkman, 2007; Jonkman, 2009a) to enable coupled nonlinear aero-hydro-servo-elastic analysis in the time domain. Turbulent-wind inflow is prescribed by the external computer program TurbSim (Jonkman et al., 2009b). FAST and AeroDyn combined account for the applied aerodynamic and gravitational loads, the behavior of the control and protection systems, and the structural dynamics of the wind turbine. The latter contribution includes the elasticity of the rotor and tower, along with the elastic coupling between their motions and the motions of the support platform.

Nonlinear restoring loads from the mooring system are obtained from a quasi-static mooring-line module that accounts for the elastic stretching of an array of homogenous taut or slack catenary lines with seabed interaction. The HydroDyn platform hydrodynamics module accounts for linear hydrostatic restoring; nonlinear viscous drag from incident-wave kinematics, sea currents, and platform motion; the added-mass and damping contributions from linear wave radiation, including free-surface memory effects; and the incident-wave excitation from linear diffraction in regular or irregular seas. HydroDyn requires as input hydrodynamic coefficients, including the frequency-domain hydrodynamic-added-mass and hydrodynamic-damping matrices and wave-excitation force vector. In this work, these hydrodynamic coefficients were generated using WAMIT (Lee, 2006), which uses the three-dimensional numerical-panel method to solve the linearized hydrodynamic radiation and diffraction problems for the interaction of surface waves with offshore platforms in the frequency domain.

OVERVIEW OF THE ANALYSIS SPECIFICATIONS

To obtain useful information from this conceptual design-and-analysis project, use of realistic and standardized input data is required. A large collection of input data is needed, including detailed specifications of the wind turbine and floating platforms, along with a design basis. A design basis consists of analysis methods (discussed above), a collection of applicable design standards and load cases, and the site-specific metocean parameters at a reference site. For this project, the specifications of the representative utility-scale multi-megawatt turbine known as the "NREL offshore 5-MW baseline wind turbine" were used (Jonkman et al., 2009c). The loads and stability analyses were run according to the procedures of the IEC 61400-3 offshore wind turbine design standard. A location in the northern North Sea was selected as the reference site from which to obtain metocean data (Jonkman, 2007).

Floating Platforms

Six different floating systems were modeled that support the NREL 5-MW turbine, with each of the three primary floating platform classes being represented. The systems modeled include two different TLP systems (the MIT/NREL TLP and the UMaine TLP); a spar buoy called the OC3-Hywind spar at two different water depths (the original is at 320 m and the UMaine version at 200 m); the UMaine semisubmersible; and the ITI Energy barge. All of these floating platforms were developed specifically to support the rotor, nacelle, and tower of the NREL baseline 5-MW system. Using the same turbine system in both the onshore and offshore applications has precedence because the design process prescribed in the IEC 61400–3 design standard endorses deriving a sea-based wind turbine design from that of a land-based wind turbine.

Each platform is described briefly below. The systems are illustrated in Fig. 1 and their properties are summarized in Table 1. Detailed specifications are available for the original three designs in Matha 2010 (for the MIT/NREL TLP), in Jonkman 2009d (for the OC3-Hywind spar buoy), and in Jonkman 2007 (for the ITI Energy barge).

The MIT/NREL TLP is a platform derived from modifications to a TLP designed at the Massachusetts Institute of Technology (MIT). It is a cylindrical platform, ballasted with concrete and moored by four pairs of vertical tendons in tension. Each pair of tendons attaches to a spoke that radiates horizontally from the bottom of the platform. The concrete ballast is used to ensure that the combined turbine-platform system remains stable during float-out—even without the tendons—in mild metocean conditions. Note that the platform could have been made much smaller without this design feature. The design of the NREL 5-MW wind turbine remains unchanged when mounted on the MIT/NREL TLP.

MIT/NREL TLP

UMaine TLP

OC3-Hywind Spar

UMaine Spar

ITI Energy Barge

UMaine Semi

Fig. 1. Floating wind turbine design concepts

specifications were given on how a full-scale system would be transported at sea.

The OC3-Hywind spar buoy is a platform that was developed within the Offshore Code Comparison Collaboration (OC3), which is a project that operated under Subtask 2 of the International Energy Agency (IEA) Wind Task 23. The platform imitates the spar-buoy concept called "Hywind," developed by StatoilHydro of Norway, but includes adaptations to make it both suitable for supporting the NREL 5-MW machinery and appropriate for public dissemination. The system is referred to as the "OC3-Hywind" system to distinguish it from StatoilHydro's original Hywind concept. The OC3-Hywind system features a deeply drafted, slender spar buoy with three catenary mooring lines. The lines attach to the platform via a delta connection (or "crowfoot") to increase the yaw stiffness of the moorings. The tower of the NREL 5-MW wind turbine is modified to conform to the spar, and the baseline generator-torque and blade-pitch controllers are changed to maintain positive aerodynamic damping and to minimize rotor-speed excursions when operating above rated wind speed.

The UMaine-Hywind spar is the same as the OC3-Hywind spar, with the exception that it is modeled at a depth of 200 m rather than 320 m, which requires slight modifications to the mooring system and the modes of the tower. The reason for the change in water depth is that the University of Maine demonstration project seeks to examine the response of its three generic designs at the same water depth.

The ITI Energy barge is a preliminary barge concept developed by the Department of Naval Architecture and Marine Engineering at the Universities of Glasgow and Strathclyde through a contract with ITI Energy. The barge is square and is ballasted with seawater to achieve a reasonable draft, which is not so shallow that it is susceptible to incessant wave slamming. To prevent it from drifting, the platform is moored by a system of eight slack, catenary lines. Two of these lines emanate from each corner of the bottom of the barge such that they are 45° apart at the corner. When the NREL 5-MW wind turbine is mounted on the ITI Energy barge, the gains in the baseline blade-pitch controller are detuned to maintain positive aerodynamic damping when operating above rated wind speed.

The UMaine semisubmersible is a generic model of a semisubmersible created for the University of Maine DeepCwind project. It consists of a main column attached to the tower and three offset columns that are connected to the main column through a series of smaller diameter pontoons. Each column starts above the still water line and continues beneath the water, with an overall platform draft of 20 m. Catenary mooring lines are attached near the base of each of these columns. The size and weight of this design are much larger than the other systems. Like the barge, the semisubmersible relies mainly on waterplane area to achieve stability. But, unlike the barge, it also has a fairly deep draft and ballasting for further stabilization. The same controller was used for this system as was used for the spars, since the platform-pitch frequencies of these systems are similar.

Load Cases

A loads and stability analysis was performed for each of the seven models, using the IEC 61400-3 offshore wind turbine design standard as a guide. Table 2 summarizes the applied DLCs. In this table, the DLCs are indicated for each design situation by wind condition, wave condition, operational behavior of the control system, fault scenarios, and other events. For the land-based cases, the wave conditions were discarded and the tower was cantilevered to the ground at its base.

The UMaine TLP is a much smaller and lighter system compared to the MIT/NREL TLP. It also has a cylindrical platform that is ballasted, but has only three legs that protrude from this base. Tensioned vertical tendons extend from the tips of each of the legs to the sea bed, to which they are anchored. The total tension in these cables due to excess buoyancy in the system is less than half the tension in the MIT/NREL TLP. The hub height is the same for both TLP systems (87.6 m), but the tower properties were modified to conform to the UMaine TLP. The controller for the two TLP systems is the same, and is the one used for the land-based system as well. The UMaine TLP was created for a demonstration project out of the University of Maine, which will build a 1/50th scale version and test the system in a wave basin. No

Table 1. Summary of properties for the six floating platforms

	MIT/NREL TLP	UMaine TLP	OC3-Hywind Spar Buoy	UMaine-Hywind Spar Buoy	ITI Energy Barge	UMaine Semi-Submersible
Water Depth (m)	200	200	320	200	150	200
Diameter or width × length (m)	18	6.5 (column) 15 (tank)	6.5 to 9.4 (tapered)	6.5 to 9.4 (tapered)	40 × 40	50 (col. spacing) 6.5 (main col.) 12 (offset col.)
Draft (m)	47.89	24	120	120	4	20
Water displacement (m^3)	12,180	2,767	8,029	8,029	6,000	13,990
Mass, including ballast (kg)	8,600,000	774,940	7,466,000	7,466,000	5,452,000	13,547,000
CM location of the platform below SWL (m)	40.61	19.72	89.92	89.92	0.2818	13.74
Roll inertia about CM($kg \cdot m^2$)	571,600,000	150,780,000	4,229,000,000	4,229,000,000	726,900,000	9,139,000,000
Pitch inertia about CM ($kg \cdot m^2$)	571,600,000	150,780,000	4,229,000,000	4,229,000,000	726,900,000	9,139,000,000
Yaw inertia about CM ($kg \cdot m^2$)	361,400,000	98,850,000	164,200,000	164,200,000	1,454,000,000	16,170,000,000
Number of mooring lines	8 (4 pairs)	3	3	3	8	3
Depth to fairleads, anchors	47.89 200	28.5 200	70 320	70 200	4 150	14 200
Radius to fairleads, anchors (m)	27 27	30 30	5.2 853.9	5.2 445	28.28 423.4	40.87 837.6
Unstretched line length (m)	151.7	171.4	902.2	468	473.3	835.4
Line diameter (m)	0.127	0.222	0.09	0.09	0.0809	0.0766
Line mass density (kg/m)	116	302.89	77.71	145	130.4	113.4
Line extensional stiffness (N)	1,500,000,000	7,720,000,000	384,200,000	384,200,000	589,000,000	753,600,000

Simulations considering power production under normal operation throughout a range of wind and wave conditions are considered in the 1.x-series DLCs. The 2.x-series DLC considers power production with fault occurrences, each of which triggers a shutdown of the turbine. The 6.x- and 7.x-series DLCs consider parked (idling) and idling with fault scenarios, respectively, under extreme 1- and 50-year return periods. The start-up, normal shutdown, and emergency shutdown events of DLCs 3.x, 4.x, and 5.x—as well as the 8.x-series cases that relate to transport, assembly, maintenance, and repair—are neglected. In Table 2, NTM and ETM refer to the normal and extreme turbulence models, ECD refers to the extreme coherent gust with direction change, EWS refers to extreme wind shear, EOG refers to the extreme operating gust, EWM refers to the extreme wind model, and NSS and ESS refer to the normal and extreme sea states. The IEC 61400-3 standard explains the DLC prescriptions and nomenclature in detail (IEC, 2008). Jonkman 2007 provides the specifics of how the DLC prescriptions were carried out in this project.

Although the IEC 61400-3 standard explicitly states that "the design requirements specified in this standard are not necessarily sufficient to ensure the engineering integrity of floating offshore wind turbines", for the purposes of this project (which principally is a conceptual study), the stated design requirements were assumed to be sufficient. No attempt was made to identify other possible floating platform-specific design conditions.

To account for all of the combinations of wind conditions, wave conditions, and control scenarios—together with the number of required seeds—2,190 separate time-domain simulations were run for each offshore floating wind turbine model, and 452 separate simulations were run for the land-based turbine model. Each simulation involving a discrete wind event—for DLCs 1.4, 1.5, and 2.3—was 1 minute long. Each simulation involving an ESS—for DLCs 1.6, 6.x, and 7.1a—was 1 hour long. All other simulations—for DLCs 1.1, 1.2, 1.3, and 2.1—lasted 10 minutes. An additional 30 seconds of simulation time (in addition to the times listed) was processed before outputting simulation data to eliminate any start-up transient behavior that may have otherwise spuriously affected the response predictions.

For the ultimate-type (U) simulations, extreme-event tables were generated for each DLC; these tables then were concatenated to find the overall ultimate (maximum) load across all DLCs. Load partial safety factors (PSF) were applied in this process to weight each DLC properly, as indicated in the last column of Table 2. The IEC 61400-3 standard requires that the ultimate loads predicted for the RNA in DLC 1.1 under normal operation with normal wind-turbulence and stochastic-wave conditions be based on the statistical extrapolation of the load response. To simplify the analysis, we eliminated this extrapolation and instead applied an extra factor of 1.2 to all load measures in all models. (The factor of 1.2 is based on the authors' experience with loads extrapolation but should be considered as an approximation because the extrapolation will—in general—depend on the turbine configuration, environmental conditions, and load measure.) Furthermore, DLC 1.1 was applied to the loads in both the RNA and the floating support structures despite the IEC 61400-3 standard only requiring DLC 1.1 to apply to the RNA.

Table 2. Summary of selected design load cases

DLC	Winds		Waves			Controls / Events	Type	Load Factor
	Model	Speed	Model	Height	Direction			
1) Power Production								
1.1	NTM	$V_{in} < V_{hub} < V_{out}$	NSS	$H_s = E[H_s|V_{hub}]$	$\beta = 0°$	Normal operation	U	1.25×1.2
1.2	NTM	$V_{in} < V_{hub} < V_{out}$	NSS	$H_s = E[H_s|V_{hub}]$	$\beta = 0°$	Normal operation	F	1.00
1.3	ETM	$V_{in} < V_{hub} < V_{out}$	NSS	$H_s = E[H_s|V_{hub}]$	$\beta = 0°$	Normal operation	U	1.35
1.4	ECD	$V_{hub} = V_r, V_r \pm 2m/s$	NSS	$H_s = E[H_s|V_{hub}]$	$\beta = 0°$	Normal operation; ±Δ wind dir'n.	U	1.35
1.5	EWS	$V_{in} < V_{hub} < V_{out}$	NSS	$H_s = E[H_s|V_{hub}]$	$\beta = 0°$	Normal operation; ±Δ ver. & hor. shr.	U	1.35
1.6a	NTM	$V_{in} < V_{hub} < V_{out}$	ESS	$H_s = 1.09 \times H_{s50}$	$\beta = 0°$	Normal operation	U	1.35
2) Power Production Plus Occurrence of Fault								
2.1	NTM	$V_{hub} = V_r, V_{out}$	NSS	$H_s = E[H_s|V_{hub}]$	$\beta = 0°$	Pitch runaway → Shutdown	U	1.35
2.3	EOG	$V_{hub} = V_r, V_r \pm 2m/s, V_{out}$	NSS	$H_s = E[H_s|V_{hub}]$	$\beta = 0°$	Loss of load → Shutdown	U	1.10
6) Parked (Idling)								
6.1a	EWM	$V_{hub} = 0.95 \times V_{50}$	ESS	$H_s = 1.09 \times H_{s50}$	$\beta = 0°, \pm30°$	Yaw = 0°, ±8°	U	1.35
6.2a	EWM	$V_{hub} = 0.95 \times V_{50}$	ESS	$H_s = 1.09 \times H_{s50}$	$\beta = 0°, \pm30°$	Loss of grid → -180° < Yaw < 180°	U	1.10
6.3a	EWM	$V_{hub} = 0.95 \times V_1$	ESS	$H_s = 1.09 \times H_{s1}$	$\beta = 0°, \pm30°$	Yaw = 0°, ±20°	U	1.35
7) Parked (Idling) and Fault								
7.1a	EWM	$V_{hub} = 0.95 \times V_1$	ESS	$H_s = 1.09 \times H_{s1}$	$\beta = 0°, \pm30°$	Seized blade; Yaw = 0°, ±8°	U	1.10

For the fatigue-type (F) simulations (DLC 1.2), instead of applying the full long-term joint-probability distribution of wind speed, significant wave height, and peak-spectral wave period, we assumed that the fatigue loads could be reasonably calculated using only the expected value of the significant wave height conditioned on mean hub-height wind speed, $E[H_s, V_{hub}]$, together with the median peak spectral period associated with each significant wave height. For these fatigue simulations, lifetime damage-equivalent loads (DEL) were calculated according to the process given in the IEC design standards. This process involves (1) binning the cycle ranges and means of each load time series by a rainflow-cycle counting (RCC) algorithm, (2) transforming the load ranges with varying means to equivalent load ranges at a fixed, mean load, (3) extrapolating the short-term cycle counts to 20-year lifetime-equivalent cycle counts, and (4) computing the lifetime DEL. In this process, the load ranges were transformed from varying to fixed mean loads using a Goodman correction with a range of assumed ultimate strengths. The ultimate strengths were derived by scaling-up the ultimate loads from the land-based loads analysis. The extrapolation for the lifetime-equivalent cycle counts used a Rayleigh probability distribution for the wind speeds. The lifetime DEL was calculated using a range of Wöhler material exponents appropriate to each component. Matha 2010 explains the fatigue-processing approach of this project in detail, with the clarification that the fixed mean load used for scaling was a value of zero.

RESULTS AND DISCUSSION

Loads analyses for each of the seven system models were run according to the specifications, data, and procedures described above. Due to the sheer volume of results, only a small fraction can be presented here. The results presented focus on the characteristic responses of each system and the system-to-system comparisons. Greater detail is available in Jonkman 2007 for the land-based NREL 5-MW wind turbine and the ITI Energy barge system, and in Matha 2010, and Jason and Matha 2010 for the MIT/NREL TLP system and the comparison of

the original three floating wind systems. No further details have been published for the University of Maine systems.

To gain insight into the dynamic behavior of the onshore and floating systems—and to enable a meaningful comparison between them—the results were split into groups which are presented separately here. First, the ultimate loads from DLCs 1.1, 1.3, 1.4, and 1.5, which consider the wind turbine in normal operation with a variety of external wind and wave conditions—not including extreme 1- or 50-year events—are presented. Next the fatigue loads from DLC 1.2 are presented. These two sets of results embody the response of the systems unencumbered by the design problems that will be discussed next.

Other load cases that were analyzed include DLCs 1.6a, 2.x, 6.x, and 7.1a, which are concerned with the wind turbine when it is experiencing a fault, when it is idling, and when it is being excited by 1-year and 50-year wind and wave conditions. These load cases produced wind turbine loadings that were unacceptably large, and therefore were not included in the ultimate load and fatigue analyses. Instead, these load cases were used to identify potential problems in the system configurations, including the presence of instabilities in all of the floating systems. A discussion of these instabilities is provided in Jonkman and Matha 2010 for the original three configurations, and will not be repeated here. The new University of Maine configurations demonstrate the same instabilities as the original concepts, and therefore a new discussion is not warranted.

Ultimate Loads

The absolute extreme loads from the extreme-event tables (the absolute maximum values of the minima and maxima) of DLCs 1.1, 1.3, 1.4, and 1.5 were calculated. The resulting loads from the six floating wind turbine systems were divided by the corresponding absolute extremes from the land-based turbine's analysis. The resulting dimensionless ratios quantify the impact of installing an NREL 5-MW wind turbine on each of the floating platforms. These ratios are presented in Fig. 2 for the transverse bending moments of the blade root, of the low-speed

shaft at the main bearing, of the yaw bearing, and of the tower base. (Each transverse bending moment was calculated by taking the vector sum of the bending moments about the member's transverse axes.)

A ratio of unity implies that the ultimate load is unaffected by the dynamic couplings between the turbine and the floating platform in the presence of combined wind and wave loading. Ratios greater than unity imply an increase in load or response that might have to be addressed by modifying the system designs (e.g., strengthening a turbine component if the sea-based loads exceed the land-based design margins) in subsequent analysis iterations. The comparison shows that in general, the floating wind turbines show increased loads on turbine components as compared to the land-based system.

For the land-based wind turbine, many of the greatest loads on the blades and shaft were generated by the ECD events of DLC 1.4. The extreme turbulence of DLC 1.3—particularly for mean wind speeds near rated speed—played a significant role in driving most of the other large loads in the system, including the loads in the tower. This is a result of a peak in rotor thrust at rated wind speed, which is characteristic of a pitch-to-feather-controlled wind turbine.
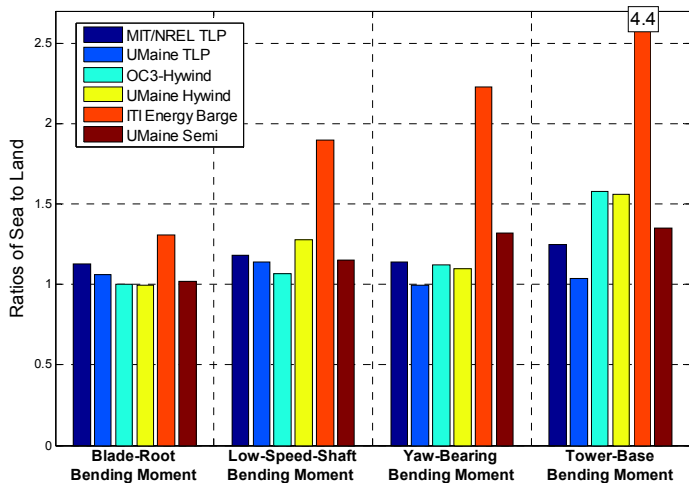
Fig. 2. Sea-to-land ratios of ultimate loads from DLCs 1.1, 1.3, 1.4, and 1.5

The wind turbine mounted on the ITI Energy barge was affected more by the waves than by the wind. Consequently, DLC 1.1 for the ITI Energy barge system—which has the greater effective partial safety factor for loads—dominated the load results more than did DLC 1.3, which has greater levels of wind turbulence but has the same wave conditions. The excessive pitching and rolling motions of the barge bring about load excursions in the supported wind turbine that exceed those experienced by the turbine installed on land. The load excursions become more extreme farther down the load path—from the blade, through the drivetrain and nacelle, to the tower—because of the increased effect of inertia from the barge-pitch motion. The loads are further exacerbated by greater yaw errors between the nominal wind direction and the rotor axis in the ITI Energy barge system as compared to the land-based system. Greater yaw errors allow for more excitation in the side-to-side direction because there is little aerodynamic damping. The greater yaw errors are generated by the yaw motion of the barge. That motion is excited by a gyroscopic yaw moment resulting from the spinning inertia of the rotor in combination with the pitching motion of the barge. Greater yaw motions are generated because of the yaw compliance of the mooring system.

The MIT/NREL TLP system has much less platform motion than the ITI Energy barge in all modes, but particularly in pitch and roll. The ultimate blade and shaft loads in the MIT/NREL TLP system for the most part were generated by the same DLC that produced the ultimate blade and shaft loads in the land-based wind turbine (DLC 1.4). The loads in the MIT/NREL TLP-supported wind turbine are slightly greater than those of the land-based turbine due to the limited platform motions that do remain. These platform-motion-induced loads cause the design-driving load case to change to DLC 1.1 for the MIT/NREL TLP-based tower as compared to DLC 1.3 for the land-based tower.

The UMaine TLP behaves very similarly to the MIT/NREL TLP. The ultimate blade and shaft loads were also generated by DLC 1.4, but had a slightly lower value than the MIT/NREL TLP, though still larger than the land-based system. The decrease in load on the shaft and blades for this TLP comes from the fact that it is also surging in the down-wind direction during the occurrence of the gust in DLC 1.4, which is what generates the extreme load for this case. This surge motion results in a decrease in the relative wind speed seen at the blades, thus reducing the load. The MIT/NREL TLP also has some surge motion, but it is less at the time of the gust, and is in the up-wind direction. This surge motion persists even after the system has reached a steady-state, and therefore, unless the gust can be applied at the same phase in the surge oscillations, the surge motion will alter the effect of the gust between the two TLP systems. This difference in initial conditions at the start of a transient event is an issue for load case simulations for floating offshore systems, and should be addressed during the creation of standards specific to floating systems. Another noticeable difference between the two TLP systems is in the extreme tower loads at the yaw-bearing and base. The extreme value of the yaw-bearing moment is caused by load case 1.3 for the UMaine TLP, rather than load case 1.4. The effect of the wind gust in DLC 1.4 does not produce as large of a load increase for the UMaine TLP, due to a combination of the differences in the surge and yaw motion of the systems. The UMaine TLP has much lower inertia and its mooring system is under less tension due to lower excess buoyancy than the MIT/NREL TLP, and thus allows for more motion in the yaw direction as well as the other platform degrees of freedom, with the exception of pitch.

The OC3-Hywind spar system has much less pitch and roll motion than that of the ITI Energy barge system, but it has much greater pitch and roll motions than the TLP systems. In regards to yaw, the OC3-Hywind spar system is more stable than the TLPs. This yields generally greater loads in the OC3-Hywind system than in the TLP systems, except for loads primarily affected by platform yaw. The load increases, however, are somewhat compensated by the modifications to the OC3-Hywind system's controller, which trades reduced blade and shaft loading with greater power and speed excursions (not shown). These modifications actually led to lower turbine loads relative to TLPs in some components. The controller, however, was modeled based on the platform-pitch frequency of the system in an undisplaced position. During rated wind speeds, it was found that the thrust of the rotor creates a large offset in the surge direction, which effectively lowers the platform-pitch frequency of the system below the designed control frequency. This results in a temporary controller-induced instability in the platform-pitch mode when the surge displacement is large. For future analyses, the frequency of the controller should be lowered to a value less than the platform-pitch frequency of any possible operational configuration. As compared with the land-based system, DLC 1.4 had much less influence on the blades in the OC3-Hywind system due to the changes in the turbine control system. Instead, most of the ultimate loads in the OC3-Hywind system were driven by DLC 1.3.

The UMaine-Hywind system, which models the spar buoy at a depth of 200 m, is very similar to the OC3 version, which is at a depth of 320 m. The only significant difference between the systems is the extreme load for the low speed shaft, which increases slightly in the UMaine system. The extreme load in the low speed shaft occurs for both spar systems in the same high turbulence event (from DLC 1.3) when there is a sudden increase in the wind speed in conjunction with a decrease in the amount of wind shear across the rotor. The magnitude of this load is tied to the pitching and surge motion of the system, and is not significant for the TLP, semisubmersible, or land-based systems. The reason the load is higher for the spar in shallower water is not fully understood, but is related to the degree to which the system is pitched during the dynamic shear event.

The motion of the UMaine semisubmersible system (semi) is most similar to the motion of the spar systems, with the exception of its heave motion, which is much larger, and its pitch motion, which is smaller. The sensitivity of the system in the heave direction can be seen by the dominance of high-period wave simulations as the design-driving load cases, especially for the low speed shaft and yaw bearing moments. The heave period for the system is approximately 17 seconds, with peak periods of the wave spectra topping out at 18.3 seconds. The increased heave motion of the system as compared to the spar results in a slight increase in the ultimate loads seen throughout the system due to increased inertial loading, with the exception of the tower-base bending moment. The tower-bending moment is largely influenced by the pitching motion of the system, which is smaller for the semi than the spars, and outweighs the effects of the heave motion. The largest increase in the ultimate load due to the heave motion of the semi can be seen in the yaw-bearing moment. The design load cases which cause the highest loads in the semi are also very similar to the spar, with the extreme turbulence of DLC 1.3 dominating.

Fatigue Loads

Fig. 3 presents the ratios calculated by dividing the lifetime DELs for the six investigated floating wind turbine concepts by the corresponding lifetime DELs from the land-based analysis. Ratios are given for the in-plane and out-of-plane blade-root bending moments, the 0° and 90° low-speed-shaft bending moments at the main bearing, and the side-to-side and fore-aft bending moments in the yaw bearing and in the tower base. Each DEL is computed using multiple Wöhler material exponents (m). For the composite blade, the DELs are computed using m equal to 8, 10, and 12. For the steel shaft and tower, the DELs are computed using m equal to 3, 4, and 5. Although the DELs also were calculated using a range of ultimate strengths, Fig. 3 presents only the results calculated with the greatest ultimate strengths applied. (The DELs asymptotically approach a constant value as the ultimate strength is increased; see Matha 2010).

In general, the fatigue load ratios show similar trends to those of the ultimate load ratios, and are produced by the same physics explained for the ultimate loads. The fatigue loads of the ITI Energy barge-supported wind turbine are by far the greatest for all of the concepts—particularly for the blade and tower. The out-of-plane blade-root bending fatigue loads in the spar systems and semi are, perhaps surprisingly, less than those of the land-based system. This is a result of the controller modification in the semi and spar systems, which—as stated above—trades reduced blade and shaft loading for greater power and speed excursions. The differences in the fatigue loads between the TLP systems and the semi and spar systems are not significant, except for the fatigue loads of the tower base, which are greater in the semi and spar systems due to their increased motion in roll and pitch. The pitch motion of the semi is less than that of the spar, and so the fatigue

at the tower-base in the fore-aft direction is less as well as the blade-root out-of-plane bending moment. The fatigue loads for the UMaine TLP system in general increase slightly compared to the NREL/MIT TLP system due to the increased platform motion, with the exception of pitch. The exception is the out-of-plane blade-root bending moment and the fore-aft tower bending moment, which are both influenced by the pitching motion of the system. The increased stiffness of the mooring lines of the UMaine TLP decreases the pitch motion in the system, which results in decreased fatigue loads associated with the pitching motion.

CONCLUSIONS

The results presented in this work characterize the dynamic responses of six different floating wind turbine concepts, represented here by the MIT/NREL TLP, the UMaine TLP, the OC3-Hywind spar buoy, the UMaine-Hywind spar buoy, the ITI Energy barge system, and the UMaine semisubmersible, together with the NREL 5-MW baseline wind turbine. The impacts brought about by the dynamic coupling between the turbine and each floating platform are presented, and comparisons between the concepts are quantified. In summary, all of the floating wind turbines show increased loads on turbine components as compared to the land-based system, and therefore must be strengthened. The platform motion-induced ultimate and fatigue loads for all turbine components in the ITI Energy barge are the highest found for these six concepts. The designs for the two TLP systems were very different, but it was found that their response was fairly similar. This shows that the method for stabilizing the floating system is more influential on the dynamics of the system than the details of the design. The differences in the ultimate and fatigue loads between the TLP systems and the spar and semi systems are not significant, except for the loads in the tower, which are less for the TLP systems. The modeling of the OC3-Hywind system at a shallower depth did not have a significant effect on the system dynamics.

One issue discovered during these simulations is the effect of platform motion in the floating systems on the resulting extreme loads. New standards with load cases specifically designed for floating systems are now being created. This issue should be addressed when developing the appropriate load case scenarios. For instance, the extreme load from a transient event could be assessed by simulating the transient event at a variety of onset times. This would address the influence of the alignment of the transient event with a specific phase of the platform motion.

These results will help resolve the fundamental design trade-offs between the floating system concepts. Although the present results quantify the extent by which the choices in platform configuration impact the turbine loads and ultimately the turbine design, without further considerations (especially economic), no definite statement can yet be made about which concept or hybrid thereof is likely the "best." Therefore, future work will be focused on cost modeling, model improvement, and the analysis of other floating wind turbine concepts. To improve the UMaine models, data from the scaled model tests of these concepts will be examined. This data will be used to validate the UMaine models, and better understand the limitations of the simulation tools being used.

ACKNOWLEDGEMENTS
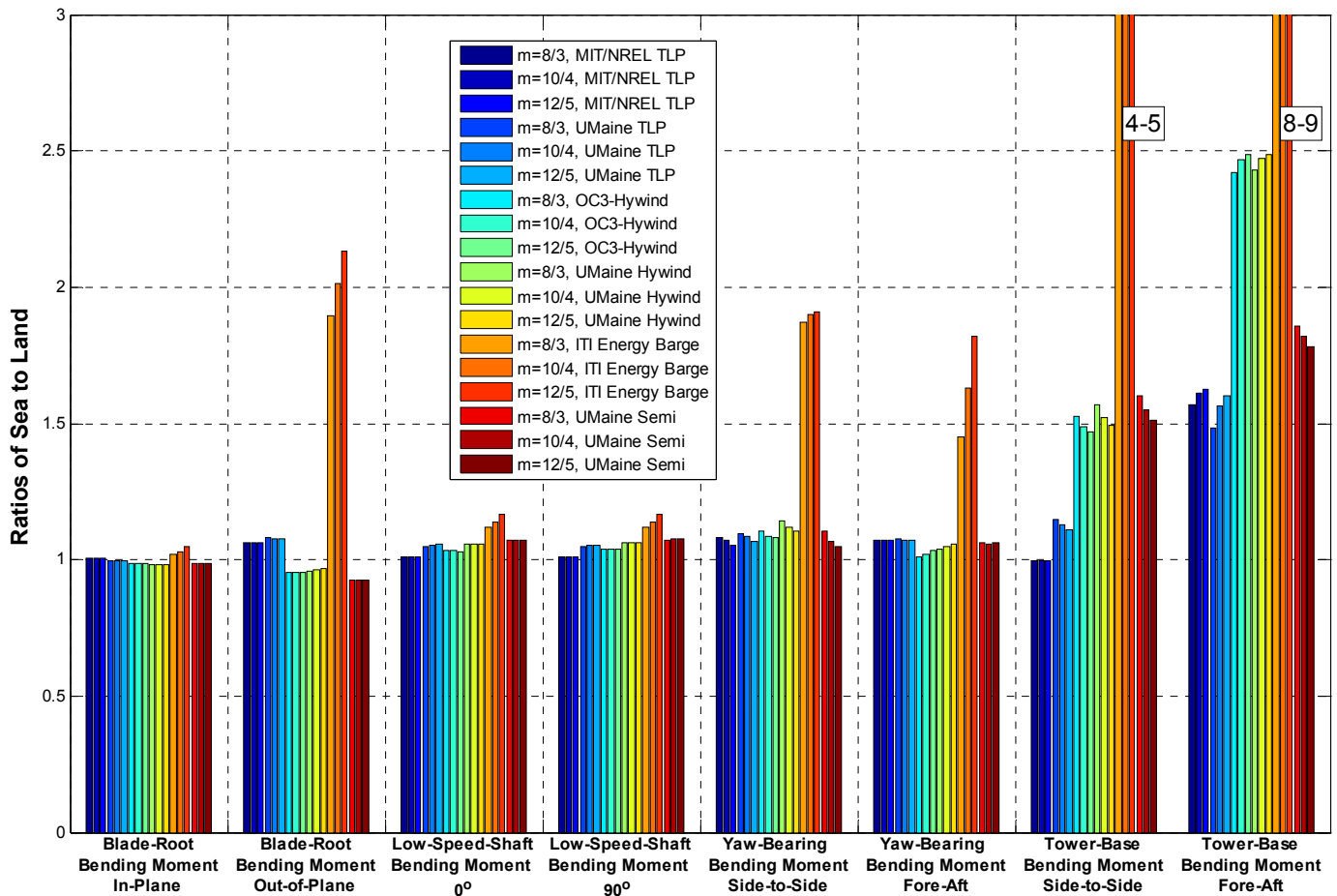
Fig. 3. Sea-to-land ratios of fatigue loads from DLC 1.2

REFERENCES

IEC (2008). *IEC 61400–3 Ed. 1. Wind Turbines – Part 3: Design Requirements for Offshore Wind Turbines*.

Jonkman, JM, and Buhl, ML Jr. (2005). *FAST User's Guide*. NREL/EL-500-38230 (previously NREL/EL-500-29798). NREL: Golden, CO.

Jonkman, JM (2007). *Dynamics Modeling and Loads Analysis of an Offshore Floating Wind Turbine*. PhD Thesis, Department of Aerospace Engineering Sciences, University of Colorado, Boulder, CO, 2007. [Online]. Available: http://www.nrel.gov/docs/fy08osti/41958.pdf (Accessed 26 May 2010)

Jonkman, JM (2009a). "Dynamics of Offshore Floating Wind Turbines—Model Development and Verification," *Wind Energy*, Vol 12, pp 459-492.

Jonkman, BJ, and Buhl, ML Jr. (2009b). *TurbSim User's Guide*, NREL/EL-500-46198 (previously NREL/EL-500-41136). NREL: Golden, CO, 2009.

Jonkman, J, Butterfield, S, Musial, W, and Scott, G (2009c). *Definition of a 5-MW Reference Wind Turbine for Offshore System Development*. NREL/TP-500-38060. NREL: Golden, CO.

Jonkman, J (2009d). *Definition of the Floating System for Phase IV of OC3*. NREL/TP-500-47535. NREL: Golden, CO.

Jonkman, JM, and Matha, D (2010). "Dynamics of offshore floating wind turbines − analysis of three concepts," *Wind Energy*, Accepted and Printing Pending, DOI: 10.1002/we.442; NREL/JA-500-48495. Golden, CO: National Renewable Energy Laboratory.

Laino, DJ, and Hansen, AC (2002). *User's Guide to the Wind Turbine Dynamics Aerodynamics Computer Software AeroDyn*. Windward Engineering LLC: Salt Lake City, UT, 2002.

Larsen, TJ, and Hanson, TD (2007). "A Method to Avoid Negative Damped Low Frequent Tower Vibrations for a Floating, Pitch Controlled Wind Turbine," *Journal of Physics: Conference Series, The Second Conference on The Science of Making Torque From Wind*, Copenhagen, pp 28–31 August 2007; DOI:10.1088/1742-6596/75/1/012073.

Lee, CH, and Newman, JN (2006). *WAMIT User Manual, Versions 6.3, 6.3PC, 6.3S, 6.3S-PC*. WAMIT, Inc.: Chestnut Hill, MA.

Matha, D (2010). *Model Development and Loads Analysis of an Offshore Wind Turbine on a Tension Leg Platform, with a Comparison to Other Floating Turbine Concepts*. MS Thesis, Endowed Chair of Wind Energy, Universität Stuttgart, Germany, 2009. [Online]. Available: http://www.nrel.gov/docs/fy10osti/45891.pdf (Accessed 26 May 2010)